Anvita Bieza

FUNCTIONAL MAGNETIC RESONANCE IMAGING IN FOLLOW-UP OF CEREBRAL GLIAL TUMORS

Summary of Doctoral Thesis to obtain
PhD degree in medicine

Specialty – Diagnostic Radiology

Riga, 2013

Doctoral thesis was developed in Riga Eastern Clinical University Hospital "Gaiļezers" and Department of Radiology, Rīga Stradiņš University

Scientific supervisor:

Dr. habil. med., Professor **Gaida Krumina**,
Rīga Stradiņš University

Official reviewers:

Dr. med., Professor **A. Millers**, Rīga Stradiņš University

Dr. habil. med., Professor **I. Aksiks**, University of Latvia

Dr. med. **O. Utehina**, Riga Eastern Clinical University Hospital "Gaiļezers"

Doctoral Thesis will be defended on the 28th of June, 2013 at 14.00 at Rīga Stradiņš University open meeting of Promotion Council of Theoretical Medicine in Riga, Dzirciema Street 16, Hippocrate auditorium.

Promotion thesis is available at Rīga Stradiņš University library and home page: www.rsu.lv

The Doctoral Thesis was supported by the European Social Fund program "Support for acquisition of doctoral study program and obtaining of a scientific degree in Rīga Stradiņš University"

Secretary of the Promotional Council:

Dr. habil. med., Professor **Liga Aberberga-Augskalne**

TABLE OF CONTENTS

LIST OF ABBREVIATIONS

Cho	choline
Cr	creatine
DTI	diffusion tensor imaging
FA	fractional anisotropy
FOV	field of view
LL	lipids and lactate
MI	myo-inositol
MRI	magnetic resonance imaging
MRS	magnetic resonance spectroscopy
NAA	N-acetylaspartate
ROI	region of interest

INTRODUCTION

Glioma is the most common malignant primary tumor that arises in the brain (1,2). It accounts for approximately 70% of the malignant primary brain tumors in adults, the incidence is 6 cases per 100 000 per year (3).

Despite the development of advanced surgical technique, new methods of focused radiotherapy and novel chemotherapy schemes, the majority of glial brain tumors recur due to the invasive growth pattern (2). Even after total resection of tumor recurrence is observed near the primary tumor localization (1). Malignant infiltrative brain gliomas have tendency to infiltrate surrounding white matter for several centimeters from the core of tumor (4). Despite numerous studies, preoperative assessment of glioma invasion and resection border remains one of the major problems in neuro-oncology (5). Another important, unresolved issue is the clinical and radiological distinction of glial tumor recurrence and radiation/chemotherapy induced injury (6), as structural MRI is often nonspecific in post-treatment period – both recurrent tumor and inflammatory or necrotic changes due to radiation/chemotherapy typically accumulate contrast agents.

Noninvasive evaluation of cerebral white matter, visualization of white matter fibers, information about the tract destruction, especially in the area around the tumor is essential in diagnosis, treatment planning and determination of prognosis (1). In daily practice MRI with intravenous contrast administration is the main additional method for the initial noninvasive investigation of patients with intracranial mass. It helps to assess tumor volume, but not the extent of tumor infiltration in white matter tracts. The use of conventional structural MRI sequences is limited because of their insensitivity for detection of tumor cells outside the visible tumor border (4,7), as well as provides little functional information (8). In such cases, advanced imaging

techniques could be of great value, which allows monitoring the physiological and metabolic characteristics of the tumor and surrounding brain tissue (1).

MRS is a noninvasive imaging of metabolic changes within the brain (9). In parallel, the DTI sequence was developed in the last decade and has application in the evaluation of white matter pathways by measuring the degree and directionality of water diffusion in tissue (10).

In this study the quantitative parameter of DTI (FA) and MRS metabolic ratios (Cho/Cr, NAA/Cr, LL/Cr and MI/Cr) were measured in selected brain areas. The brain white matter tracts were reconstructed in damaged hemisphere and compared with the opposite normal hemisphere pathways using DTI 3-dimensional tractography method, color coded FA maps and color coded fiber orientation maps. So far, such multimodal approaches in glial tumors studies were not well described in the literature.

Although various studies indicate that DTI and MRS quantitative measurements can provide additional information in glial tumors diagnostics and monitoring, it is necessary to determine the repeatability of the tests so that they could be more widely used in clinical practice. However, the reproducibility of DTI and MRS derived indices has not yet been systematically analyzed in the literature (11). Even less repeatability research has been conducted from patients with glial brain tumor. This is the first study evaluating the repeatability index of FA and MRS measures in the tumor, zone of perifocal edema, as well as the distant and the contralateral symmetrical normal-appearing white matter.

The structure of the doctoral thesis:

Doctoral thesis is written in Latvian and executed on 149 pages. It has one attachment. The work has a classic design, it includes annotations in Latvian and English, introduction, topicality, novelty and practical significance of the study, the aim and the objectives of the study, hypotheses, literature review, materials and methods, results, discussion, conclusions, list of publications and

reports, bibliography which includes 173 references. Doctoral thesis contains 10 tables and 156 figures.

The aim of the study was to assess the usefulness of DTI and MRS in glial brain tumor specified primary radiological diagnosis, and in differentiation between glial tumor recurrence and radiation/chemotherapy induced changes in the brain.

Objectives:

1. Investigate **FA** changes in the specific areas of interest – tumor, zone of perifocal edema, treatment induced injury zone, the distant and the contralateral normal-appearing white matter.
2. Collect and analyze the MRS data - different **metabolites ratios** – in identical areas of interest on patients with glial tumors and treatment induced brain injury.
3. Assess the possibility of **MRI tractography** in characterization of white matter injury caused by tumor and in evaluation of applied treatment.

Hypotheses:

1. Glial brain tumor and its perifocal zone are characterized by different values and ratios of MRS neuronal markers, specific changes in brain white matter tracts and quantitative differences in diffusion anisotropy parameters that allow radiological evaluation of tumor spread in visually unchanged peritumoral area.
2. Radiation and/or chemotherapy induced brain injury and tumor recurrence is possible to differentiate, based on differences in MRS neuronal markers and diffusion anisotropy parameters.

Topicality, novelty and practical significance of the study:

1. This is the first study in Latvia to evaluate the role of MRS and DTI in glioma diagnosis and in the assessment of treatment effectiveness.
2. For the first time, multimodal approach has been used for the study of glial tumors, combining structural MRI with analysis of MRS and DTI

quantitative parameters, color coded FA maps, color coded fiber orientation maps and 3-dimensional tractography.

3. MRI tractography methodology has been approbated in clinical practice.
4. Results of this study indicate that DTI is able to differentiate between different white matter tract lesions due to the spread of glial tumor, which is important for preoperative planning and for determining treatment effectiveness.
5. This is the first study evaluating the repeatability index of FA and MRS measures in the tumor, zone of perifocal edema, as well as the distant and the contralateral symmetrical normal-appearing white matter.
6. New data were obtained about the role of MRS and DTI in determination of the vital glioma cells and infiltration area.
7. The most important MRI parameters for evaluating the effectiveness of radiation/chemotherapy were identified.
8. Several recommendations have been developed to introduce DTI and MRS in clinical practice.
9. Our MRI protocol improves the accuracy of radiological diagnosis both for newly diagnosed glioma patients and repeated examination, evaluating the efficacy and side effects of treatment. Accurate diagnosis allows choosing the most appropriate treatment, thereby improving the quality of life and prolonging survival.

Personal contribution:

The author personally participated in all stages of the research – in the study design; in the collection of material, MRI data post-processing, statistical analysis, interpretation of the results obtained, literature review, preparation of publications, theses, conferences reports, and translation; is the author of the published images.

1. MATERIALS AND METHODS

1.1. Patient selection

The study included 150 MRI examinations in 92 patients acquired during the period between August 2009 and December 2011. The study included patients with both newly diagnosed brain glioma and those in the follow-up period after treatment.

Inclusion criteria:

1. Morphologically confirmed brain glioma.
2. MRI performed using a protocol including DTI and MRS sequences.
3. High quality MRI images (without motion artifacts).

Exclusion criteria:

1. Patients without morphologically confirmed brain glioma.
2. Patients with histologically confirmed another type of pathology.
3. MRI performed using a protocol without DTI and/or MRS sequences.
4. Poor quality MRI images (with motion artifacts).

Patients were divided into **two major groups** based on histological findings and structural MRI appearance:

1. Patients with glial brain tumors.
2. Patients in remission after treatment.

73 patients were included in the first group with typical glial brain tumors. Two subgroups were categorized depending on whether or not the patient had received radiotherapy/chemotherapy: before radiotherapy/ chemotherapy (n=24), after radiotherapy/chemotherapy (n=49). The time period between initiation of radiotherapy/chemotherapy and MRS, DTI examinations were from 0.5 to 130 months. The majority of patients (n=53) had received corticosteroids before the MRI examination, 20 patients had not

received corticosteroids. Depending on grades of malignancy two subgroups were dealt: low-grade glioma (grade II) – 7 patients; high-grade glioma (grade III and IV) – 66 patients.

The second study group included 77 patients in remission with treatment induced brain injury. The treatment induced brain injury was determined by the following criteria: long-term stability of the structural MRI findings or spontaneous regression of lesions. In our study the median follow-up time was 9.41 months (range, 3 - 24 months).

1.2. Morphological and immunohistochemical examinations

The patients enrolled in this study had different types of neuroepithelial tumors: 53 glioblastomas, 42 anaplastic oligoastrocytomas, 26 anaplastic astrocytomas, 11 astrocytomas, 7 oligoastrocytomas, 5 anaplastic oligodendrogliomas, 4 oligodendrogliomas, 1 pleomorphic xanthoastrocytoma and 1 astroblastoma. Tumors were classified by using the 2007 revised World Health Organization classification of tumors of the central nervous system (12). The final histopathological diagnosis was determined by analysis of formalin-fixed, paraffin-embedded tissue samples. The standard method was hematoxylin and eosin staining, and immunohistochemical analysis, including Ki-67 antigen immunostaining (MIB-1 antibody) and GFAP (glial fibrillary acidic protein).

Tumor grade was determined histologically, based on seven criteria of malignancy: mitotic activity, microvascular proliferation - angiogenesis, necrosis in tumor, cell polymorphism, nuclear pleomorphism, cell density, lymphocytic muff around the blood vessels.

1.3. Magnetic resonance imaging protocol

All patients were examined using a 1.5 Tesla MR system (General Electric Signa EXCITE MR) equipped with an eight-channel head coil. MRI protocol included following examination sequences:

1. **Standard structural sequences**
    a. Axial T2 propeller or coronal T2 FRFSE.
    b. Axial T2 FLAIR propeller or coronal T2 FLAIR.
    c. Axial diffusion-weighted imaging (0/Ax DWI 1000b ASSET).
    d. Obl T1 3D FSPGR IR prep before and after intravenous gadolinium-based contrast media administration.
2. **DTI** (TENSOR 25 directions 1000b).
3. **MRS** was performed with 2-dimensional multi-voxel chemical shift imaging - (8ch) PROBE-2DSI PRESS 144TE.

The total MRI acquisition time was maximum 20 minutes 17 seconds.

1.4. Magnetic resonance imaging data processing

MRS and DTI primary data were automatically transferred to the workstation *MR GELS (General Electric*) for post-processing. MRS spectral curves, metabolite measurements and DTI images (color coded FA maps, color coded fiber orientation maps and 3-dimensional tractography) were obtained by using the program *Functool*.

Quantitative DTI and MRS measurements were made on identical areas of interest, which were placed manually. In the study group of typical glioma the measurements were made at four locations: tumor, zone of perifocal edema, the distant and the contralateral normal-appearing white matter. In the

second study group of patients in remission the measurements were made at three locations: abnormal signal intensity area around the postoperative cavity (treatment induced injury zone), the distant and the contralateral normal-appearing white matter. Placement of ROI was based on previously published recommendations (4).

1.4.1. Fractional anisotropy measurements

To make the measurements of quantitative DTI parameter (FA), DTI gray scale maps and color coded FA maps were reconstructed. FA measurements were made on defined areas of interest, which were placed manually on 2-dimensional DTI gray scale maps. Overall, 496 FA measurements were obtained. Selection of the ROI was based on the different brain areas which were identified by the structural T2, FLAIR, post-contrast T1 images and color coded FA maps. The ROI size for FA measurements was 30 pixels (41.2mm^2).

1.4.2. Tractography

In order to distinguish the different tract lesions, the structural MRI images, color coded FA maps, color coded fiber orientation maps and 3-dimensional tractography reconstructions were used.

Overall, 243 brain white matter tracts were reconstructed in affected hemisphere – 71 internal capsule/corona radiata, 62 subcortical U-fibers, 40 inferior longitudinal fasciculus, 28 uncinate fasciculus, 19 corpus callosum, 8

inferior frontooccipital fasciculus, 7 middle cerebellar peduncle fibers, 6 arcuate fasciculus, 2 cingulum.

In order to visualize white matter tracts by tractography, it was necessary to find the ROIs - the starting points to reconstruct the tract. In our study these starting points were placed manually on DTI color coded fiber orientation maps, based on previously developed 3-dimensional tractography atlas (13) and adapted it to our workstation. Both single and multiple ROIs were used for tractography, depending on the type of tract.

White matter tract involvement adjacent to tumor was classified as displacement, edema, infiltration and disruption according to previously published criteria (5):

- Tract displacement – tract maintained normal anisotropy relative to the corresponding tract in the contralateral hemisphere, but was situated in an abnormal location or with an abnormal orientation on color coded fiber orientation maps (5).
- Tract edema – tract maintained normal anisotropy and orientation, but demonstrated high signal intensity on T2 and FLAIR images (5).
- Tract infiltration – tract showed reduced anisotropy, but remained identifiable on color coded fiber orientation maps (5).
- Tract disruption – anisotropy was markedly reduced such that the tract could not be identified on color coded fiber orientation maps (5).

1.4.3. Magnetic resonance spectroscopy

Quantitative measurements of MRS (Cho/Cr, NAA/Cr, LL/Cr, MI/Cr ratios) were made in definite areas of interest – identical to those of FA measurements. After the automatic MRS data post-processing we determined

the highest metabolic peaks at specific points of spectral curve - MI at 3.5-3.6ppm, Cho 3.2ppm, Cr 3.0ppm and NAA 2.0ppm. Regarding LL we determined the sum of peak heights between 0.8 and 1.3 ppm. Individual voxels were placed on defined areas of interest at the previously scanned slice. Then the spectrum was calculated automatically. Each metabolite peak was initially assessed visually and metabolite ratios were calculated. Cr was used as the denominator for calculating metabolite ratios, because it is considered the most stable cerebral metabolite. Overall, 2057 measurements of metabolite ratios were obtained.

1.5. Statistical analysis

Microsoft Office Excel 2003 was used for data collection. Statistical analysis was performed by using the Statistical Package for the Social Sciences (SPSS, version 20). Statistical methods of data analysis:

1. Descriptive statistics were used for calculating the mean and standard deviations of the samples and the measures (Cho/Cr, NAA/Cr, MI/Cr, LL/Cr and FA). The Kolmogorov - Smirnov test was used to determine if the data were normally distributed.
2. Conclusive statistics:
    - Hypothesis testing. If the variables in paired samples did not meet the normal distribution ($p<0.05$), the nonparametric related samples Wilcoxon signed rank test was used to compare pairs. If the data were normally distributed ($p>0.05$), the paired sample t-test was used to compare the values of means for two related samples.
    - The repeatability of measurements was tested with single factor analysis of variance (ANOVA, MS Excel). Mean squares between

groups (MS_A) and mean squares within groups (MS_W) were derived from ANOVA. Repeatability index (r) was calculated using the following formulas:

$$r=S^2A/(S^2+S^2A) \quad \text{(1.formula)}$$

S^2 is mean square within group (MS_W).

$$S^2A = (MS_A-MS_W)/n_0 \quad \text{(2.formula)}$$

n_0 is the weighted average number of observations per group (14).

In this study we have 2 observations per individual, so $n_0=2$.

The following terminology was used to describe various degrees of repeatability as recommended Martin and Bateson (1986):

- r <0.2 – slight repeatability,
- r 0.2-0.4 – low repeatability,
- r 0.4-0.7 – moderate repeatability,
- r 0.7-0.9 – high repeatability,
- r >0.9 – very high repeatability. This repeatability index was only used in cases if data were statistically significant (15).

A p value of less than 0.05 was considered to indicate a significant difference.

2. RESULTS

After post-processing 150 MRI scans, 2553 quantitative measurements of metabolite ratios (Cho/Cr, NAA/Cr, LL/Cr, MI/Cr) and FA parameter were obtained on defined areas of interest: 362 measurements were made in the tumor, 324 measurements in the zone of perifocal edema, 380 measurements in the treatment induced injury zone, 744 measurements in the distant normal-appearing white matter and 743 measurements in the contralateral normal-appearing white matter.

2.1. Glial tumors

2.1.1. Fractional anisotropy analysis

We calculated FA mean values and standard deviations in each area of interest using descriptive statistics method. We observed a gradual increase of FA values in the direction from tumor to peritumoral zone and contralateral normal-appearing white matter. The FA measurements results (mean ± standard deviation) in patients with glial brain tumors: in the tumor 0.122(±0.049); in the perifocal edema 0.175(±0.323); in the distant normal-appearing white matter 0.323(±0.091); in the contralateral normal-appearing white matter 0.473(±0.068).

Comparing data in paired samples between tumor and perifocal edema, statistically significant differences were observed between the FA mean values ($p<0.001$, Wilcoxon test).

Comparing data in paired samples between tumor and distant normal-appearing white matter, statistically significant differences were observed between the FA mean values ($p<0.001$, Wilcoxon test).

Comparing data between tumor and contralateral normal-appearing white matter, statistically significant differences were observed between the FA mean values ($p<0.001$, Wilcoxon test).

Comparing data between perifocal edema and distant normal-appearing white matter, statistically significant differences were observed between the FA mean values ($p<0.001$, t–test).

Comparing data between perifocal edema and contralateral normal-appearing white matter, statistically significant differences were observed between the FA mean values ($p<0.001$, Wilcoxon test).

Comparing data between distant and contralateral normal-appearing white matter, statistically significant differences were observed between the FA mean values ($p<0.001$, Wilcoxon test).

To determine whether the received radiation/chemotherapy affected diffusion anisotropy parameters, we compared the measurements in two subgroups of patients - before radiotherapy/chemotherapy (n=24) and after radiotherapy/chemotherapy (n=49) by the Wilcoxon test. At any of the measured areas FA mean values did not show statistically significant difference.

To determine whether the use of corticosteroids affected FA parameters, we compared the measurements in two subgroups of patients by the Wilcoxon test - patients who received corticosteroids (n=53) and who did not receive corticosteroids (n=20) before MRI. At any of the measured areas FA mean values did not show statistically significant difference.

2.1.2. Metabolite ratio analysis

We calculated mean values and standard deviations of Cho/Cr, NAA/Cr, MI/Cr, LL/Cr ratios in each area of interest using descriptive statistics

method. There were gradual reduction of Cho/Cr, MI/Cr, LL/Cr mean ratios and gradual increase of NAA/Cr mean values in the direction from the tumor to the distant and contralateral normal-appearing white matter. The MRS measurements (NAA/Cr, Cho/Cr, MI/Cr, LL/Cr ratios) are displayed in the Table 2.1.

Table 2.1.

The metabolite measurements results (mean ± standard deviation) in patients with glial brain tumors

The metabolite ratios	Tumor	Perifocal edema	Distant normal-appearing white matter	Contralateral normal-appearing white matter
Cho/Cr	2.305(±1.543)	1.444(±0.953)	1.143(±0.545)	0.924(±0.366)
NAA/Cr	1.031(±0.517)	1.221(±0.560)	1.493(±0.767)	2.354(±1.010)
MI/Cr	0.814(±0.509)	0.756(±0.494)	0.509(±0.302)	0.482(±0.315)
LL/Cr	3.933(±1.547)	2.791(±1.313)	1.834(±0.896)	1.247(±0.427)

A clinical example of DTI and MRS quantitative measurements from a patient with glial brain tumor is demonstrated in figure (Fig.2.1.).

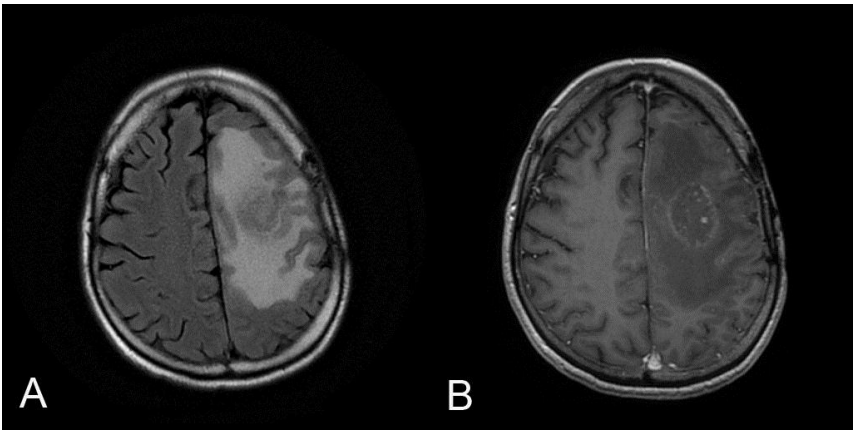

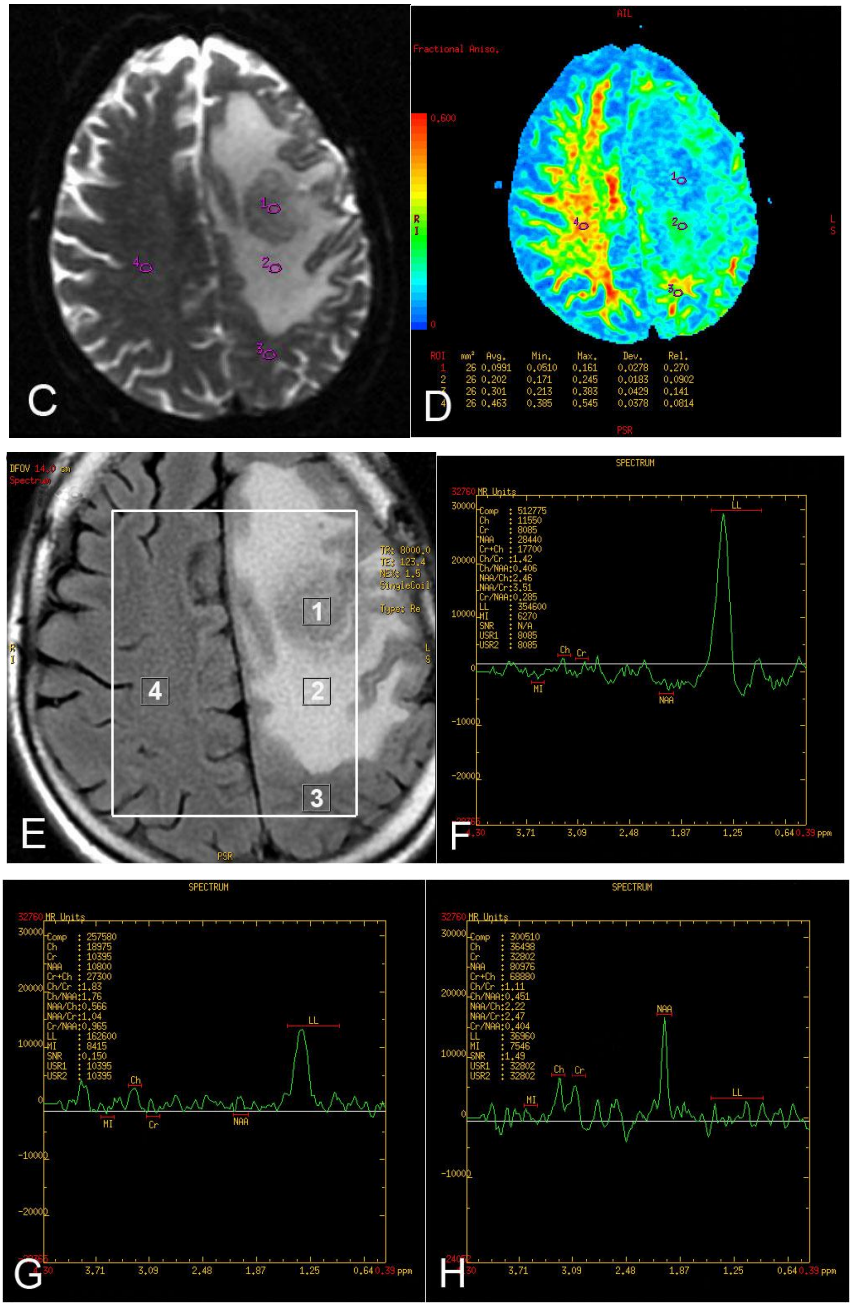
C
D
Fractional Aniso.
ROI mm² Avg. Min. Max. Dev. Rel.
1 25 0.0991 0.0510 0.161 0.0278 0.270
2 26 0.202 0.171 0.245 0.0183 0.0902
3 26 0.301 0.213 0.383 0.0429 0.141
4 26 0.463 0.385 0.545 0.0578 0.0814
E
F
SPECTRUM
32760 MR Units
Comp : 512775
Ch : 11550
Cr : 8085
NAA : 28440
Cr+Ch : 17700
Ch/Cr :1.42
Ch/NAA:0.406
NAA/Ch:2.46
NAA/Cr:3.51
Cr/NAA:0.285
LL : 354600
MI : 6270
SNR : N/A
USR1 : 8085
USR2 : 8085
G
SPECTRUM
32760 MR Units
Comp : 257580
Ch : 18975
Cr : 10395
NAA : 10800
Cr+Ch : 27300
Ch/Cr :1.83
Ch/NAA:1.76
NAA/Ch:0.566
NAA/Cr:1.04
Cr/NAA:0.965
LL : 162600
MI : 8415
SNR : 0.150
USR1 : 10395
USR2 : 10395
H
SPECTRUM
32760 MR Units
Comp : 300510
Ch : 36498
Cr : 32802
NAA : 80376
Cr+Ch : 68880
Ch/Cr :1.11
Ch/NAA:0.451
NAA/Ch:2.22
NAA/Cr:2.47
Cr/NAA:0.404
LL : 36360
MI : 7546
SNR : 1.49
USR1 : 32802
USR2 : 32802
3.71 3.09 2.48 1.87 1.25 0.64 0.39 ppm

Fig.2.1. MR images of 48 years old male with recurrent anaplastic oligodendroglioma. A. Axial FLAIR MRI shows an infiltrative left frontal lobe white matter mass with extensive perifocal edema. B. Axial T1 image after contrast administration demonstrates a well-defined solid tumor with inhomogeneous contrast enhancement and perifocal edema. C. Axial gray scale diffusion tensor map with ROIs placements for the determination of the FA values in definite areas: the tumor [1], the perifocal edema [2], the distant normal-appearing white matter [3] and the contralateral normal-appearing white matter [4]. D. Color coded FA map demonstrates gradual reduction of FA values in the direction from the periphery to the tumor. Regions of high anisotropy are shown in red, and regions of low anisotropy are shown in blue. E. The location of the MRS volume of interest in the brain is outlined by a white square. ROIs for the calculation of the metabolite ratios were placed in identical localizations. F. Typical MRS spectrum of the tumor from the ROI [1] with an elevated LL peak, reduced NAA peak. G. MRS spectrum in the perifocal edema from the ROI [2] displays reduced NAA peak and gradually reduced LL peak in comparison with tumor. H. MR spectrum in the contralateral normal-appearing white matter [4] shows high NAA peak. The LL peak is not visible. (Images from the author's archive)

Comparing data in paired samples between tumor and perifocal edema, statistically significant differences were observed between the Cho/Cr mean values ($p<0.001$, Wilcoxon test), between the NAA/Cr mean values ($p=0.009$, t–test), between the LL/Cr mean values ($p<0.001$, t–test), but MI/Cr did not show statistically significant difference ($p=0.647$, Wilcoxon test).

Comparing data in paired samples between tumor and distant normal-appearing white matter, statistically significant differences were observed between the Cho/Cr mean values ($p<0.001$, Wilcoxon test), between the NAA/Cr mean values ($p<0.001$, t–test), between the MI/Cr mean values ($p<0.001$, Wilcoxon test), between the LL/Cr mean values ($p<0.001$, Wilcoxon test).

Comparing data between tumor and contralateral normal-appearing white matter, statistically significant differences were observed between the Cho/Cr mean values ($p<0.001$, Wilcoxon test), between the NAA/Cr mean values ($p<0.001$, Wilcoxon test), between the MI/Cr mean values ($p<0.001$, Wilcoxon test), between the LL/Cr mean values ($p<0.001$, t–test).

Comparing data between perifocal edema and distant normal-appearing white matter, statistically significant differences were observed between the Cho/Cr mean values ($p=0.034$, Wilcoxon test), between the NAA/Cr mean values ($p=0.010$, t–test), between the MI/Cr mean values ($p=0.002$, Wilcoxon test), between the LL/Cr mean values ($p<0.001$, Wilcoxon test).

Comparing data between perifocal edema and contralateral normal-appearing white matter, statistically significant differences were observed between the Cho/Cr mean values ($p<0.001$, Wilcoxon test), between the NAA/Cr mean values ($p<0.001$, Wilcoxon test), between the MI/Cr mean values ($p<0.001$, Wilcoxon test), between the LL/Cr mean values ($p<0.001$, t–test).

Comparing data between distant and contralateral normal-appearing white matter, statistically significant differences were observed between the Cho/Cr mean values ($p=0.002$, Wilcoxon test), between the NAA/Cr mean values ($p<0.001$, Wilcoxon test), between the LL/Cr mean values ($p<0.001$, Wilcoxon test), but MI/Cr did not show statistically significant difference ($p=0.365$, Wilcoxon test).

To determine whether the received radiation/chemotherapy affected neuronal markers, we compared the measurements in two subgroups of patients: before radiotherapy/chemotherapy (n=24) and after radiotherapy/ chemotherapy (n=49) by the Wilcoxon test. Comparing measurements in the distant normal-appearing white matter, LL/Cr mean values before radiotherapy/chemotherapy 2.267 and after radiotherapy/chemotherapy 1.622 showed statistically significant difference ($p=0.013$). Other measurements did not show statistically significant differences. Since only the LL/Cr measurements in the distant normal-appearing white matter showed statistically significant difference in patients before and after radiotherapy/chemotherapy, we compared this measurement between patients in clinical and radiological

remission period (1.377) and patients after received combination therapy with a residual tumor tissue (1.622). The measurements did not show statistically significant difference (p=0.193).

To determine whether the use of corticosteroids affected neuronal markers, we compared the measurements in two subgroups of patients by the Wilcoxon test: patients who received corticosteroids (n=53) and who did not receive corticosteroids (n=20) before MRI. In the perifocal edema NAA/Cr mean values in the first subgroup 1.282 and in the second subgroup 1.018 showed statistically significant difference (p=0.048).

2.1.3. Tractography findings

After analysis of 3-dimensional tractography reconstructions, color coded FA maps and color coded fiber orientation maps, four main types of fiber damage by glial tumor spread were defined – displacement, edema, infiltration and disruption. These types were divided, based on fiber continuity and orientation on 3-dimensional tractography images and visual assessment of color coded FA maps and color coded fiber orientation maps. We observed tract edema in 3 patients, displacement in 21 patients, infiltration in 32 patients, disruption in 37 patients. Tract lesions were not observed in 9 patients with DTI (Table 2.2.). Tract lesions depending on the grading of malignancy are summarized in the Table 2.3. Postoperative white matter tract defect was found in 35 patients.

Table 2.2.

Characteristics of white matter tracts involvement in patients with different histological types of glial tumors

Type of involvement	Histological diagnosis	Number of white matter tracts studied
Norm (n=9)	Glioblastoma	5
	Anaplastic astrocytoma	3
	Anaplastic oligoastrocytoma	1
Edema (n=3)	Glioblastoma	1
	Oligoastrocytoma	1
	Anaplastic oligoastrocytoma	1
Infiltration (n=32)	Glioblastoma	22
	Anaplastic astrocytoma	6
	Anaplastic oligoastrocytoma	2
	Astrocytoma	1
	Oligoastrocytoma	1
Displacement (n=21)	Glioblastoma	12
	Anaplastic astrocytoma	4
	Anaplastic oligoastrocytoma	3
	Astrocytoma	1
	Oligodendroglioma	1
Disruption (n=37)	Glioblastoma	23
	Anaplastic astrocytoma	6
	Anaplastic oligoastrocytoma	4
	Oligoastrocytoma	2
	Astrocytoma	1
	Anaplastic oligodendroglioma	1

Table 2.3.

Characteristics of white matter tracts involvement in high and low grade gliomas

Type of involvement	Grading of malignancy	Number of white matter tracts studied
Norm (n=9)	high grade	9
	low grade	0
Edema (n=3)	high grade	2
	low grade	1
Infiltration (n=32)	high grade	30
	low grade	2
Displacement (n=21)	high grade	19
	low grade	2
Disruption (n=37)	high grade	34
	low grade	3

Analyzing tract anatomical division, we found the following affected tracts caused by tumor growth and spread – internal capsule/corona radiata were affected in 28 patients, inferior longitudinal fasciculus - 23, uncinate fasciculus - 16, corpus callosum - 16, subcortical U-fibers - 11, inferior frontooccipital fasciculus - 7, middle cerebellar peduncle fibers - 7, arcuate fasciculus - 6.

Analyzing different tract lesions and their combinations, we found that most patients had only one type of fiber injury. It was observed in 34 patients (disruption in 17 cases, infiltration - 9, displacement - 4, edema - 4). Two types of fiber involvement were associated in 27 patients (infiltration + disruption in 12 cases, infiltration + displacement - 9, displacement + disruption - 6). Combined three types of fiber involvement were observed in 2 patients (displacement + infiltration + disruption).

The features of different tract lesions are demonstrated in MRI – internal capsule displacement (Fig.2.2.), inferior frontooccipital fasciculus disruption (Fig.2.3.), right middle cerebellar peduncle fibers infiltration (Fig.2.4.), subcortical U-fibers edema (Fig.2.5).

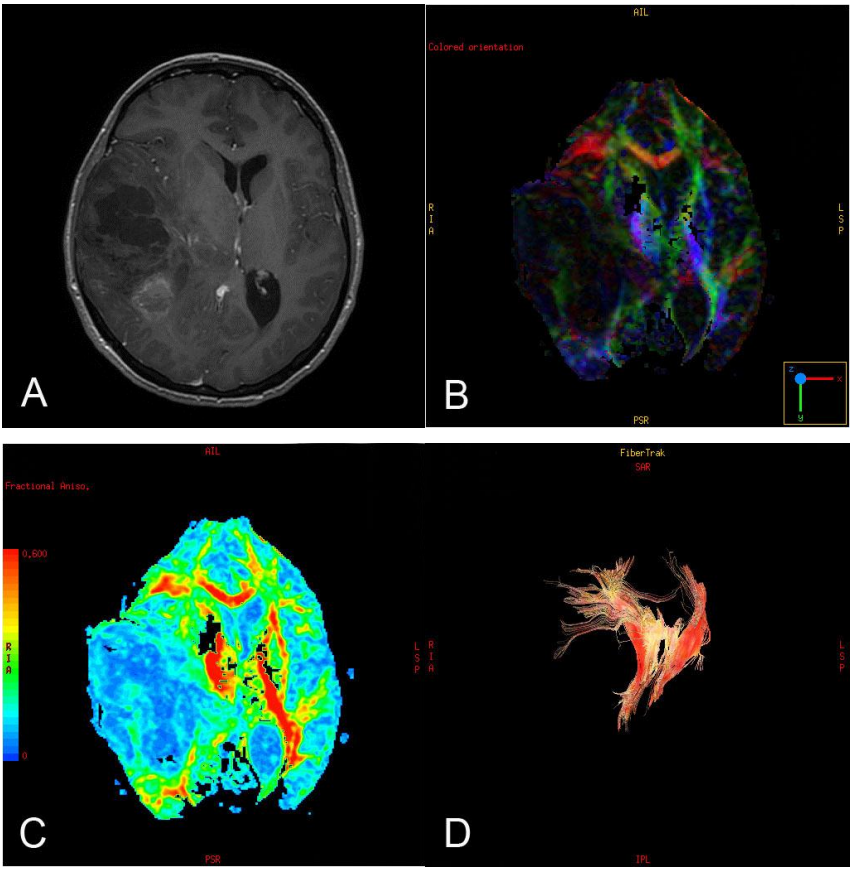

Fig.2.2. Internal capsule displacement in a 34-year-old woman with newly diagnosed anaplastic oligoastrocytoma. A. Axial T1 post-contrast MRI shows an infiltrative, inhomogeneous mass with central necrosis in the right temporal lobe, right thalamus, internal capsule with compression of right lateral ventricle and midline shift. Minimal peripheral contrast enhancement is observed. B. DTI color coded fiber orientation map demonstrates medial displacement of the posterior limb of the internal capsule; it retains normal blue-red color. C. In DTI color coded FA map the posterior limb of the internal capsule maintains normal anisotropy relative to the corresponding tract in the contralateral hemisphere. D. Coronal DTI 3-dimensional tractography reconstruction shows abnormal location of the internal capsule – it is wrapped around the tumor. (Images from the author's archive)

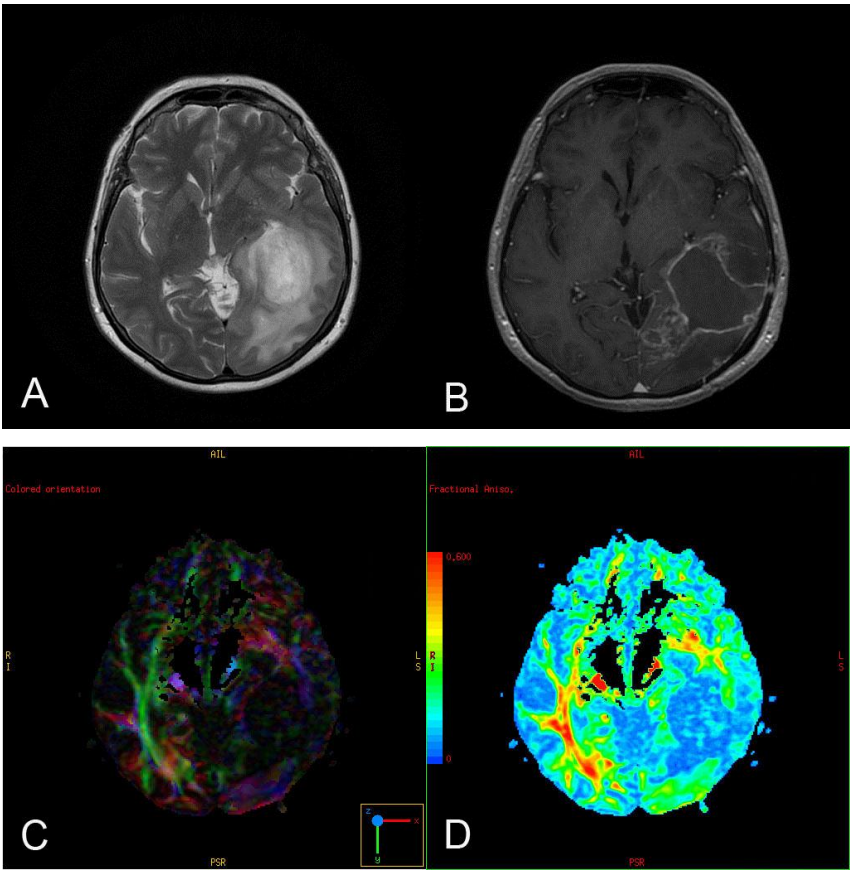

Fig.2.3. Inferior frontooccipital fasciculus disruption in a 63-year-old woman with newly diagnosed glioblastoma A. Axial T2 image shows an inhomogeneous, hyperintense mass with central necrosis in the left temporal-occipital lobe. Surrounding hyperintensity represents edema and/or tumor cells. The underlying sulci are effaced and the left ventricle is compressed. B. Axial T1 post-contrast MRI shows heterogeneous, peripheral contrast enhancement that surrounds central necrosis. C. The left inferior frontooccipital fasciculus could not be identified on DTI color coded fiber orientation map, suggestive of disruption. D. DTI color coded FA map demonstrates markedly reduced anisotropy in tumor zone. Disrupted tract could not be reconstructed with 3-dimensional tractography. (Images from the author's archive)

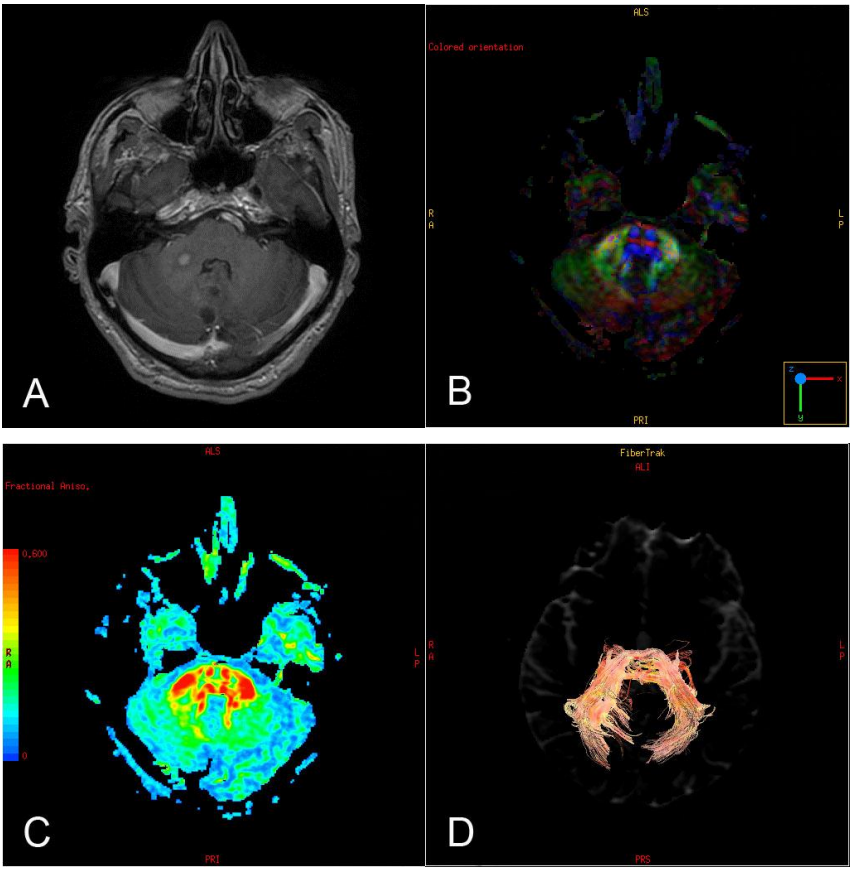

Fig.2.4. Right middle cerebellar peduncle fibers infiltration in a 62-year-old man due to residual glioblastoma tissues 2 weeks after tumor resection from the posterior cranial fossa. A. Axial T1 post-contrast MRI shows round, enhancing mass in the right middle cerebellar peduncle. B. The majority of the right middle cerebellar peduncle fibers are identifiable on DTI color coded fiber orientation map; small defect is observed in the area of lesion. C. Residual tumor shows reduced anisotropy on DTI color coded FA map. D. Axial DTI 3-dimensional tractography reconstruction demonstrates preserved cortico-ponto-cerebellar pathways. (Images from the author's archive)

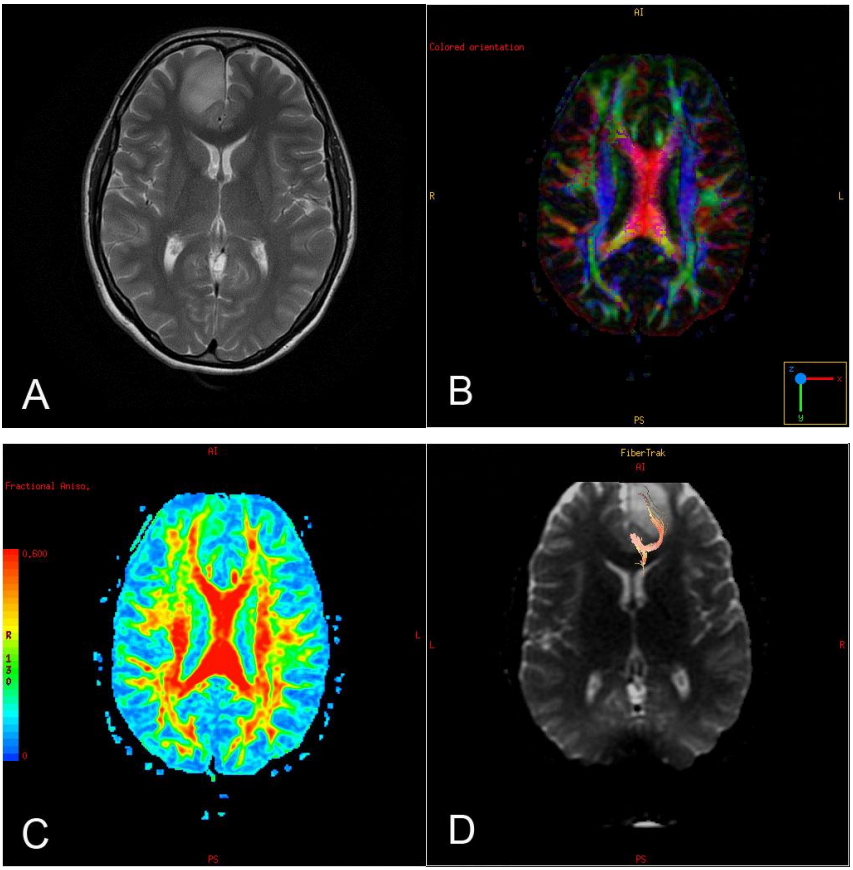

Fig.2.5. Subcortical U-fibers edema in a 25-year-old woman with newly diagnosed anaplastic oligoastrocytoma. A. Axial T2 image shows a hyperintense mass in the right frontal lobe. B. Tract is maintained normal orientation on DTI color coded fiber orientation map. C. Normal anisotropy is maintained on DTI color coded FA map, suggestive of edema. D. Axial DTI 3-dimensional tractography reconstruction (inferior view) demonstrates preserved subcortical U-fibers in the tumor area. (Images from the author's archive)

In the study group of glial brain tumors 24 patients with high-grade gliomas were followed up by repeated DTI scans to monitor for therapeutic response. The majority of patients (n=21) demonstrated tract changes in follow-up images. Tumor growth progression with signs of possible malignant transformation was observed most frequently (n=13): the white matter tract

displacement, edema or infiltration transformed into disruption, or additional tract involvement joined. More rare DTI tractography did not changed in follow-up studies (n=3) or tumor regression was seen where tracts infiltration decreased in size; their fiber orientation and color were normalized in comparison with MRI before the specific treatment (n=3). During the observation period a number of patients (n=5) underwent surgery and affected tracts were operated. Tractography findings during the follow-up period are summarized in graph (Fig.2.6.). Summarizing the results, most of glial tumor underwent malignant transformation (Fig.2.7.).

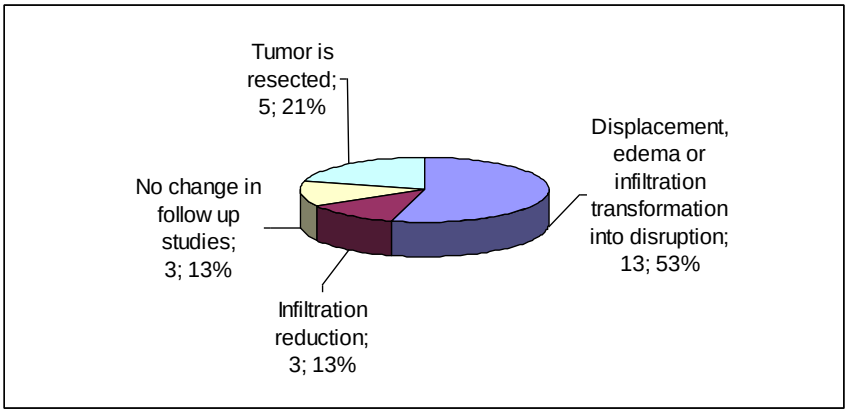

Fig.2.6. Monitoring of therapeutic response in 24 patients with high-grade cerebral gliomas using DTI tractography

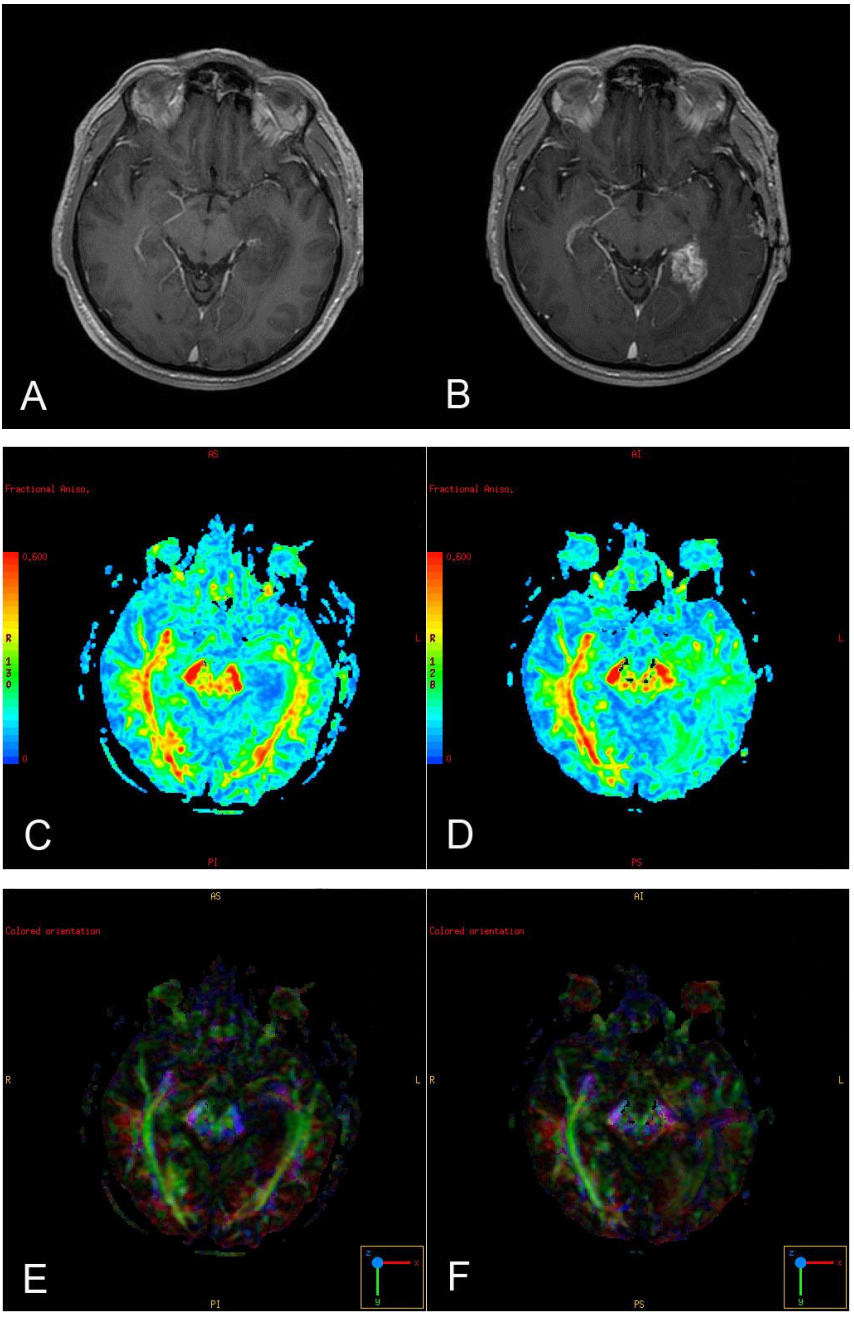
A
B
RS
Fractional Aniso.
0,800
R
120
0
L
PI
C
AI
Fractional Aniso.
0,800
R
120
0
L
PS
D
RS
Colored orientation
R
L
PI
E
AI
Colored orientation
R
L
PS
F

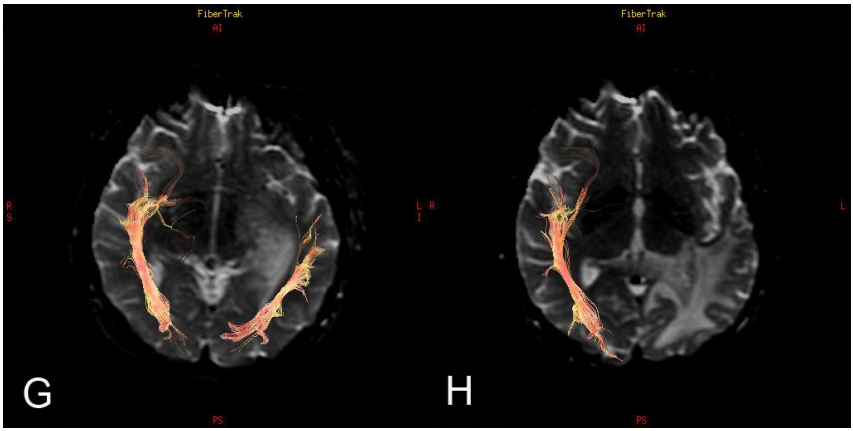

Fig.2.7. Development of high-grade tumor – tumor areas with tract infiltration and displacement undergo malignant transformation into disruption within six months in a 57-year-old man with recurrent glioblastoma. A. Axial T1 post-contrast MRI shows mild enhancement of residual tumor. B. Within six months strongly enhanced high-grade tumor is developed. C. DTI color coded FA map shows reduced anisotropy (yellow) in left inferior longitudinal fasciculus, suggestive of an infiltration. D. In a follow-up examination tract demonstrates pronounced FA reduction (greenish-blue color), suggestive of a disruption. E. Left inferior longitudinal fasciculus has maintained its normal green color on DTI color coded fiber orientation map, but it is displaced laterally by the residual tumor. F. After six months disrupted fibers of left inferior longitudinal fasciculus are no longer identifiable on DTI color coded fiber orientation map. G. Axial DTI 3-dimensional tractography reconstruction demonstrates displacement of left inferior longitudinal fasciculus. H. Disrupted left inferior longitudinal fasciculus could not be reconstructed with DTI tractography method. (Images from the author's archive)

2.2. Treatment induced brain injury

2.2.1. Fractional anisotropy analysis

We calculated FA mean values and standard deviations in each area of interest using descriptive statistics method. We observed a gradual increase of FA mean values in the direction from abnormal signal intensity area around the postoperative cavity to the distant and contralateral normal-appearing white matter. The FA measurements results (mean ± standard deviation) in patients

with treatment induced injury: in the abnormal signal intensity area around the postoperative cavity 0.185(±0.065); in the distant normal-appearing white matter 0.431(±0.058); in the contralateral white matter 0.446(±0.049).

Using a nonparametric related sample Wilcoxon signed rank test we observed statistically significant differences in FA measurements between treatment induced injury zone and distant normal-appearing white matter ($p<0.001$), between distant and contralateral normal-appearing white matter ($p<0.001$). Using a paired samples t-test, we observed statistically significant differences in FA measurements between treatment induced injury zone and contralateral normal-appearing white matter ($p<0.001$).

2.2.2. Metabolite ratio analysis

We calculated mean values and standard deviations of Cho/Cr, NAA/Cr, MI/Cr, LL/Cr ratios in each area of interest using descriptive statistics method. The results of metabolite measurements are displayed in the Table 2.4.

Table 2.4.

The metabolite measurements results (mean ± standard deviation) in patients with treatment induced injury

The metabolite ratios	Abnormal signal intensity area around the postoperative cavity	Distant normal-appearing white matter	Contralateral normal-appearing white matter
Cho/Cr	1.355(±0.606)	1.193(±0.418)	1.061(±0.432)
NAA/Cr	1.153(±0.507)	1.890(±0.705)	2.272(±0.725)
MI/Cr	0.607(±0.362)	0.452(±0.230)	0.383(±0.235)
LL/Cr	2.304(±1.213)	1.377(±0.556)	1.217(±0.353)

There were gradual reduction of Cho/Cr, MI/Cr, LL/Cr mean ratios and gradual increase of NAA/Cr mean values in the direction from the

abnormal signal intensity area around the postoperative cavity to the distant and contralateral normal-appearing white matter**.**

Using a nonparametric related sample Wilcoxon signed rank test we observed statistically significant differences in **Cho/Cr** measurements between treatment induced injury zone and distant normal-appearing white matter ($p=0.023$), between distant and contralateral white matter ($p=0.044$). Statistically significant differences in **NAA/Cr** measurements were observed between treatment induced injury zone and distant normal-appearing white matter ($p<0.001$), between treatment induced injury zone and contralateral white matter ($p<0.001$), between distant and contralateral white matter ($p<0.001$); in **MI/Cr** measurements were observed between treatment induced injury zone and distant white matter ($p<0.001$), between treatment induced injury zone and contralateral white matter ($p<0.001$), between distant and contralateral white matter ($p=0.035$); in **LL/Cr** measurements were observed between treatment induced injury zone and distant white matter ($p<0.001$), between treatment induced injury zone and contralateral white matter ($p<0.001$). LL/Cr measurements did not show statistically significant difference between distant and contralateral white matter ($p=0.054$). Using t-test, we observed statistically significant differences in **Cho/Cr** measurements between treatment induced injury zone and contralateral white matter ($p=0.001$).

2.2.3. Tractography findings

Two main types of treatment induced white matter injury were determined using 3-dimensional tractography reconstructions, color coded FA maps and color coded fiber orientation maps - post-surgical fiber defect (Fig.2.8.) and radiation/chemotherapy related demyelination destruction (Fig.2.9.).

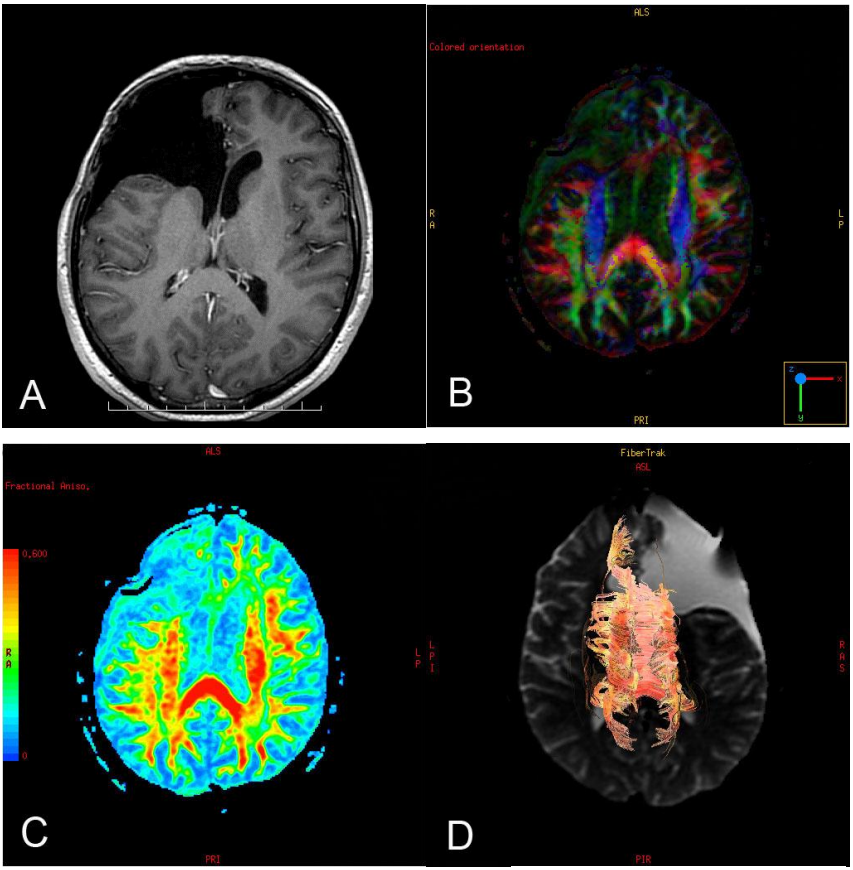

Fig.2.8. Post-surgical corpus callosum defect in a 39-year-old man after anaplastic astrocytoma surgery 4 years ago, followed by radiation and chemotherapy. A. Axial T1 post-contrast MRI shows porencephalic cavity in the right frontal lobe, which connects to the frontal horn of the right lateral ventricle. Postoperative defect is visible in the right side of genu corporis callosum, in the left side - gliosis without mass effect. Abnormal contrast enhancement is not seen. B. Genu corporis callosum in the right side is not visualized on DTI color coded fiber orientation map, in the left side - partially visualized. C. Genu corporis callosum in the right side shows significantly reduced anisotropy (blue as cerebrospinal fluid) on DTI color coded FA map, in the right side gliotic area anisotropy is moderately reduced (green). D. In the postoperative defect corpus callosum fibers are not visible, other fibers are preserved on axial DTI 3-dimensional tractography reconstruction (inferior view). (Images from the author's archive)

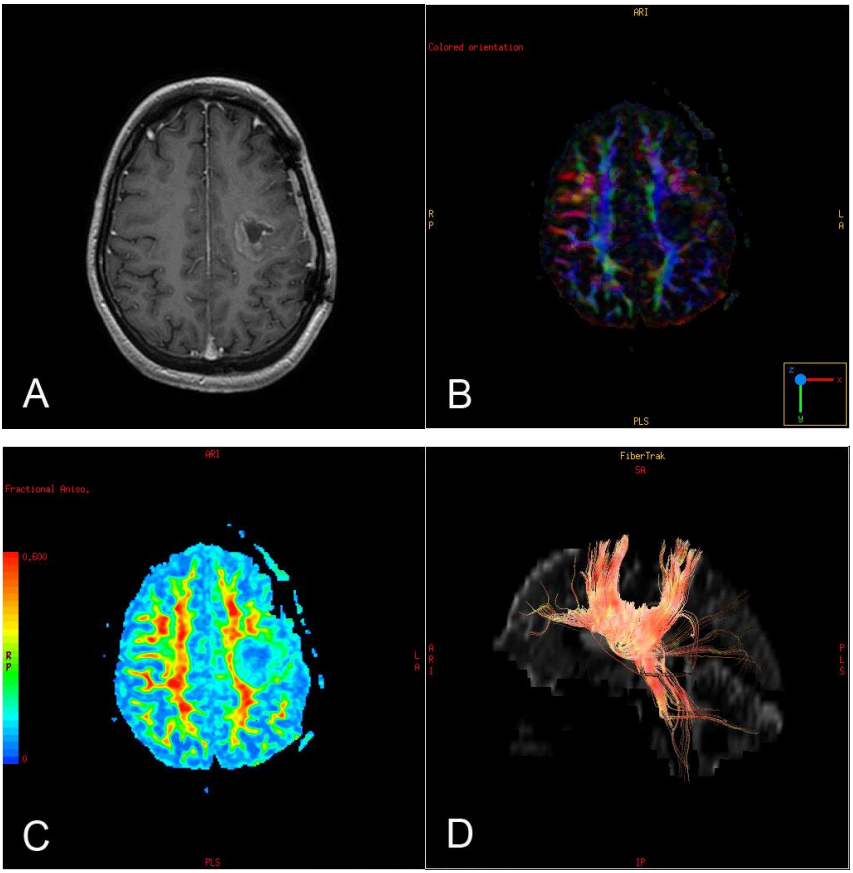

Fig.2.9. Acute radiation injury in a 44-year-old woman 2 months after anaplastic astrocytoma resection followed by radiotherapy. A. Axial T1 post-contrast MRI demonstrates postoperative cavity in the left frontal parietal lobe with a rim of contrast enhancement. Observing this area after 7 months, pathological contrast enhancement disappeared, suggesting post-treatment changes. B. Left corona radiata fibers is not visualized in the postoperative defect and perifocal abnormal signal intensity area on DTI color coded fiber orientation map. C. DTI color coded FA map shows significantly reduced anisotropy (blue) in the postoperative area, compared with the unchanged right corona radiata (red). Around the postoperative cavity an area with a slightly higher anisotropy (blue-green) is observed, where the injured brain tissue are observed on structural MRI images. D. Sagittal DTI 3-dimensional tractography reconstruction shows defect in corona radiata fibers. (Images from the author's archive)

In our study postoperative white matter tract defect was found in 71 patients, radiation/chemotherapy induced demyelination destruction in 40 patients (in 33 patients - only postoperative defect, in 2 patients - only demyelination destruction, in 38 patients - both types of fiber injury). Demyelination or gliosis around the postoperative cavity on T2 and FLAIR images were observed in all cases of varying degrees. Destruction of myelin fibers were found in 40 patients (55%) on DTI images, while in the remaining 33 patients (45%) the fibers were not affected, despite the changes on structural conventional MRI.

Analyzing tract anatomical division, we found following white matter tract lesions after treatment – in 46 patients subcortical U-fibers were affected, 38 internal capsule/corona radiata, 9 inferior longitudinal fasciculus, 3 uncinate fasciculus, 3 corpus callosum, 1 inferior frontooccipital fasciculus and 1 middle cerebellar peduncle fibers.

Postoperative fiber injury was mostly diagnosed in association and projection fibers. Postoperative defect of commissural fibers was observed in only two cases.

In this study group, 16 patients in remission were observed during follow-up period, by repeated MRI scans. In 14 cases tractography findings were not changed (control MRI was performed within 3-19 months). White matter destruction had progressed only in 2 cases (in 5 and 7 months).

2.3. Comparison of metabolites and FA between patients with glial tumors and treatment induced brain injury

Using nonparametric Wilcoxon test or t-test (depending on the data distribution), mean metabolites ratios and FA values were compared between tumor and treatment induced brain injury zone, between distant normal-

appearing white matter in patients with glial tumors and patients in remission after treatment, between contralateral normal-appearing white matter in patients with glial tumors and patients in remission.

Mean Cho/Cr, MI/Cr, LL/Cr ratios in glial brain tumors were statistically significantly higher and mean FA value lower than those in the treatment induced brain injury zone. NAA/Cr ratios between the tumor and treatment induced brain injury zone did not show statistically significant difference (Table 2.5.).

Table 2.5.

Comparison of metabolites and FA between glial tumor and treatment induced brain injury zone

Metabolites ratios and FA measurement	Tumor	Abnormal signal intensity area around the postoperative cavity	p value (test)
Cho/Cr	2.305(±1.543)	1.355(±0.606)	p<0.001 (Wilcoxon test)
NAA/Cr	1.031(±0.517)	1.153(±0.507)	p=0.192 (t-test)
MI/Cr	0.814(±0.509)	0.607(±0.362)	p=0.010 (Wilcoxon test)
LL/Cr	3.933(±1.547)	2.304(±1.213)	p<0.001 (Wilcoxon test)
FA	0.122(±0.049)	0.185(±0.065)	p<0.001 (Wilcoxon test)

Comparing measurements of distant normal signal intensity areas, NAA/Cr ratio and mean FA value were significantly lower and LL/Cr ratio was significantly higher in patients with glial tumors than those in remission period (Table 2.6.).

Table 2.6.

Comparison of metabolites and FA in the distant normal-appearing white matter between patients with glial tumors and patients in remission after treatment

Metabolites ratios and FA measurement	Distant white matter in patients with glial tumors	Distant white matter in remission	p value (test)
Cho/Cr	1.143(±0.545)	1.193(±0.418)	p=0.466 (Wilcoxon test)
NAA/Cr	1.493(±0.767)	1.890(±0.705)	p=0.002 (Wilcoxon test)
MI/Cr	0.509(±0.302)	0.452(±0.230)	p=0.130 (Wilcoxon test)
LL/Cr	1.834(±0.896)	1.377(±0.556)	p=0.001 (Wilcoxon test)
FA	0.323(±0.091)	0.431(±0.058)	p<0.001 (Wilcoxon test)

Comparing measurements of contralateral normal signal intensity areas, Cho/Cr ratio was significantly lower and MI/Cr ratio, mean FA value were significantly higher in patients with glial tumors than those in remission period (Table 2.7.).

Table 2.7.

Comparison of metabolites and FA in the contralateral normal-appearing white matter between patients with glial tumors and patients in remission after treatment

Metabolites ratios and FA measurement	Contralateral white matter in patients with glial tumors	Contralateral white matter in remission	p value (test)
Cho/Cr	0.924(±0.366)	1.061(±0.432)	p=0.045 (Wilcoxon test)
NAA/Cr	2.354(±1.010)	2.272(±0.725)	p=0.985 (Wilcoxon test)
MI/Cr	0.482(±0.315)	0.383(±0.235)	p=0.027 (Wilcoxon test)
LL/Cr	1.247(±0.427)	1.217(±0.353)	p=0.644 (t-test)
FA	0.473(±0.068)	0.446(±0.049)	p=0.017 (Wilcoxon test)

2.4. Analysis of diagnostic test accuracy

2.4.1. Repeatability of MRS and DTI measurements

To perform the repeatability analysis of DTI and MRS quantitative measurements, 20 patients with glial tumors were selected. The metabolite ratios (Cho/Cr, NAA/Cr, LL/Cr, MI/Cr) and FA measurements were repeatedly measured using the identical methodology – ROIs were placed on the tumor, zone of perifocal edema, the distant and the contralateral normal-appearing white matter. Overall, 398 repeated measurements were made.

Analyzing repeated measurements in 20 patients, statistically significant differences were not observed in the tumor between Cho/Cr measurements (p=0.180, Wilcoxon test), NAA/Cr measurements (p=0.081, t-test), MI/Cr measurements (p=0.789, t-test), FA measurements (p=0.671, t-test); in the he perifocal edema between Cho/Cr measurements (p=0.273, Wilcoxon test), MI/Cr measurements (p=0.285, Wilcoxon test), LL/Cr measurements (p=0.347, t-test), FA measurements (p=0.755, t-test); in the distant normal-appearing white matter between NAA/Cr measurements (p=0.500, Wilcoxon test), MI/Cr measurements (p=0.686, Wilcoxon test), LL/Cr measurements (p=0.528, t-test), FA measurements (p=0.563, t-test); in the contralateral normal-appearing white matter between Cho/Cr measurements (p=0.577, t-test), LL/Cr measurements (p=0.093, Wilcoxon test).

In six cases, repeated measurements were statistically significantly different, so the repeatability index r was measured. Table 2.8. shows summary of the repeatability index analysis for repeated measurements of MRS and DTI derived measures.

Table 2.8.

Results of repeatability in MRS and DTI derived measurements on 20 patients with glial brain tumors. Mean squares, F and critical values of F were derived from single factor analysis of variance (MS Excel)

Measurement	LL/Cr tumor	NAA/Cr edema	Cho/Cr distant	NAA/Cr contra-lateral	MI/Cr contra-lateral	FA contra-lateral
Mean square between groups	4.836	0.448	0.193	1.468	0.211	0.019
Mean square within groups	0.851	0.077	0.031	0.365	0.037	0.007
F ratio*	5.679	5.839	6.253	4.023	5.727	2.779
Critical value of F	2.137	2.137	2.137	2.137	2.182	2.137
p	<0.001	<0.001	<0.001	0.002	<0.001	0.01
Index of repeatability (r)	0.701	0.707	0.724	0.602	0.702	0.462
Repeatability	High	High	High	Moderate	High	Mode-rate

* F is calculated as the ratio of mean square between groups divided by mean square within groups

2.4.2. Influence of ROI size on FA measurements

To assess the influence of ROI size on FA measurements, we made repeated measurements with ROI of 12 pixels and 30 pixels in 7 different areas in 115 patients.

FA mean value in **tumor,** measured by 12 pixels ROI was 0.147(± 0.068), with a 30 pixels ROI was 0.134(±0.049) (number of measurements in each group - 50). Measurements did not show statistically significant difference (p=0.322, Wilcoxon test).

FA mean value in **zone of perifocal edema,** measured by 12 pixels ROI was 0.177(±0.063), with a 30 pixels ROI was 0.179(±0.049) (number of measurements in each group - 45). Measurements did not show statistically significant difference (p=0.803, t-test).

FA mean value in **abnormal signal intensity area around the postoperative cavity,** measured by 12 pixels ROI was 0.177(±0.098), with a 30 pixels ROI was 0.182(±0.066) (number of measurements in each group - 65). Measurements did not show statistically significant difference (p=0.133, Wilcoxon test).

FA mean value in **the distant normal-appearing white matter around the postoperative cavity,** measured by 12 pixels ROI was 0.464(±0.113), with a 30 pixels ROI was 0.432(±0.051) (number of measurements in each group - 65). Statistically significant differences were observed between the both groups (p=0.018, Wilcoxon test).

FA mean value in **the distant normal-appearing white matter on patients with glial brain tumor,** measured by 12 pixels ROI was 0.442(±0.096), with a 30 pixels ROI was 0.333(±0.099) (number of measurements in each group - 50). Statistically significant differences were observed between the both groups (p<0.001, t-test).

FA mean value in **the contralateral normal-appearing white matter on patients in remission period,** measured by 12 pixels ROI was 0.532(±0.077), with a 30 pixels ROI was 0.442(±0.047) (number of measurements in each group - 65). Statistically significant differences were observed between the both groups (p<0.001, t-test).

FA mean value in **the contralateral normal-appearing white matter on patients with glial brain tumor,** measured by 12 pixels ROI was 0.524(±0.0643), with a 30 pixels ROI was 0.473(±0.074) (number of measurements in each group - 50). Statistically significant differences were observed between the both groups (p<0.001, t-test).

3. CONCLUSIONS

1. MRS and DTI quantitative measurements in glioma peritumoral area revealed pathological changes, despite the normal signal intensity on structural MRI.
2. MRS and DTI in combination with structural MRI examination sequences enhance vital glial tumor cells areas and possible infiltration border.
3. Increased LL/Cr ratios and decreased FA values have superior implications in detecting glial tumors extent along the white matter tracts. NAA/Cr reduction and Cho/Cr increase may provide additional diagnostic value.
4. LL/Cr ratio in distal normal signal intensity area could be used as radiation/chemotherapy effectiveness criteria, as this will reduce after the received treatment and in remission stage.
5. Using a combination of structural MRI, DTI color coded FA maps, color coded fiber orientation maps and tractography method, it is possible to distinguish between different white matter tract lesions, to consider the possible malignant transformation of gliomas and evaluate the treatment effect.

4. PRACTICAL RECOMMENDATIONS

The measurement results must be accurate, repeatable, so they can be used for follow-up in determining the distribution of glial tumors and evaluating the results of treatment and disease progression. We consider several conditions relevant when performing MRS and DTI measurements from the different zones of pathological and normal brain tissues in clinical practice. First, select the appropriate slice for MRS examination; it must include the tumor, the perifocal edema area, as well as the distant and the contralateral normal white matter. Second, the MRS plane must be consistent with the DTI selected image slice for FA measurements. Third, choose the same plane in repeated MRI scans for follow-up dynamics after the treatment. Fourth, the selected ROIs for both MRS and DTI measurements must be localized in the identical areas. Fifth, one must be very accurate when conducting measurements in the normal contralateral cerebral hemisphere – it is recommended to use DTI color coded FA maps for ROI selection, which visualize the areas of white matter with different fiber connectivity. Comparative measurements must be done in the areas of normal white matter with similar FA values. Sixth, an accurate methodology and multimodal approach should be used to reconstruct tracts – combining structural MRI with DTI color coded FA maps, color coded fiber orientation maps and 3-dimensional tractography method. Seventh, the repeated measurements should be performed by one experienced neuroradiologist to avoid errors due to the subjective interpretation.

5. PUBLICATIONS AND PRESENTATIONS ON RESEARCH THEME

Publications (scientific articles) on research theme:

1. Anvita Bieza, Gaida Krumina, Daina Apskalne, Oskars Rasnacs. Magnetic resonance spectroscopy for evaluation of brain glioma extent. Acta Chirurgica Latviensis 2011;11:50-55.
2. Anvita Bieza, Gaida Krumina. Magnetic resonance tractography in follow-up of glial tumors. Collection of Scientific papers 2010. Research articles in medicine & pharmacy 2011;106-114.
3. Anvita Bieza, Gaida Krumina. Magnetic resonance study on fractional anisotropy and neuronal metabolites ratios in peritumoral area of cerebral gliomas. Medicina (Kaunas) 2012;48(10):497-506.
4. Anvita Bieza, Gaida Krumina. The value of magnetic resonance spectroscopy and diffusion tensor imaging in characterization of gliomas growth patterns and treatment efficiency. J. Biomedical Science and Engineering 2013;6:518-526.
5. Anvita Bieza, Gaida Krumina. The value of magnetic resonance in differentiation between brain glioma and treatment induced injury. Acta Chirurgica Latviensis 2012;12:24-28.

Congress abstracts on research theme:

1. Anvita Bieza, Gaida Krumina. Usefulness of MR spectroscopy in differentiation between recurrent/residual brain glioma and post-therapeutic changes. ESMRMB 2012 Congress. October 4–6, Lisbon/PT. Book of Abstracts. EPOS™ Poster / Paper Poster / Clinical Review Poster / Software Exhibits DOI: 10.1007/s10334-012-0324-9. EPOS^{TM} Poster Nr.528. Pg.398-399.

2. Anvita Bieza, Gaida Krumina. Functional magnetic resonance imaging in differentiation between glial brain tumor recurrence and treatment effects. Riga Stradins University 2012 Scientific Conference. Abstracts, pg.256.
3. Anvita Bieza, Gaida Krumina. Relationship between white matter tract changes and neurological status during treatment and surveillance of glial brain tumors. ESMRMB 2011 Congress. October 6-8, Leipzig/DE. Book of Abstracts. EPOS^{TM} Posters / Paper Posters / Clinical Review Posters / Software Exhibits. DOI: 10.1007/s10334-001-0268-5. EPOS^{TM} Poster Nr.407. Pg.289.
4. Anvita Bieza, Gaida Krumina. Brain tractography changes after glial tumor treatment. Riga Stradins University 2011 Scientific Conference. Abstracts, pg.280.
5. A.Bieza, G.Krumina. Structural changes of association, projection and commissural fibers after radiation therapy in patients with glial tumors. Electronic Presentation Online System (EPOS TM) of the European Society of radiology. www.myyESR.org/epos, DOI: 10.1594/ecr2011/C-0644
6. Anvita Bieza, Gaida Krumina. Magnetic resonance tractography in the diagnosis of cerebral gliomas. Riga Stradins University 2010 Scientific Conference. Abstracts, pg. 247.

Presentations on research theme:

1. 13.12.2012. oral report - Anvita Bieza „MRS and DTI role in characteristics of glioma growth type and treatment effects. The main results of the doctoral thesis", meeting of the Latvian Association of Neuroradiology.
2. 04.10.2012. electronic poster - Anvita Bieza, Gaida Krumina „Usefulness of MR spectroscopy in differentiation between recurrent/residual brain

glioma and post-therapeutic changes*",* European Society for Magnetic Resonance in Medicine and Biology Congress 2012, Lisbon/Portugal.

3. 30.03.2012. poster presentation - Anvita Bieza, Gaida Krumina "Functional magnetic resonance imaging in differentiation between glial brain tumor recurrence and treatment effects", Riga Stradins University 2012 Scientific Conference.
4. 06.10.2011. electronic poster - Anvita Bieza, Gaida Krumina „Relationship between white matter tract changes and neurological status during treatment and surveillance of glial brain tumors", European Society for Magnetic Resonance in Medicine and Biology Congress 2011, Leipzig, Germany.
5. 15.04.2011. poster presentation - Anvita Bieza, Gaida Krumina "Brain tractography changes after glial tumor treatment", Riga Stradins University 2011 Scientific Conference.
6. 03.03.2011. electronic poster - A. Bieza, G. Krumina „Structural changes of association, projection and commissural fibers after radiation therapy in patients with glial tumors", 23rd European Congress of Radiology, Vienna, Austria.
7. 19.03.2010. oral report - Anvita Bieza „Magnetic resonance tractography in the diagnosis of cerebral gliomas", Riga Stradins University 2010 Scientific Conference.

6. ACKNOWLEDGMENTS

I am very grateful to my scientific supervisor Professor Gaida Krumina for insightful discussions and comments, for support in collecting the study material.

Thanks to Professor Uldis Teibe, Oskars Rasnacs and Irena Rogovska for help in statistical data analysis.

I thank Juris Novozilovs, Aigars Kiecis, Liga Maurisa, Dace Saule, Ieva Berke, Irina Dovgopolika, Julija Pavaine for support in collecting the study material.

I am deeply grateful to Daina Apskalne for the carefully conducted morphological analyses and oral consultations.

I thank Laura Ziemane for technical assistance.

I wish to thank Janis Upmalis, Andris Norko, Anita Sterna, Sandra Meskovska, Rita Gudele, and Irena Badovska for the responsiveness during doctoral studies.

This study was supported by European Social Fund in Latvia (grant number 2009/0147/1DP/1.1.2.1.2/09/IPIA/ VIAA/009).

7. LIST OF REFERENCES

1. Nelson SJ. Assessment of therapeutic response and treatment planning for brain tumors using metabolic and physiological MRI. NMR Biomed 2011;24(6):734-49.
2. Wright AJ, Fellows G, Byrnes TJ, Opstad KS, McIntyre DJO, Griffiths JR, Bell BA, Clark CA, Barrick TR, Howe FA. Pattern recognition of MRSI data shows regions of glioma growth that agree with DTI markers of brain tumor infiltration. Magn Reson Med 2009;62:1646–51.
3. Ricard D, Idbaih A, Ducray F, Lahutte M, Xuan KH, Delattre JY. Primary brain tumours in adults. The Lancet 2012;379(9830):1984-96.
4. Wang W, Stewarda CE, Desmonda PM. Diffusion tensor imaging in glioblastoma multiforme and brain metastases: the role of p, q, L, and fractional anisotropy. Am J Neuroradiol 2009;30:203-8.
5. Yen PS, Teo BT, Chiu CH, Chen SC, Chiu TL, Su CF. White matter tract involvement in brain tumors: a diffusion tensor imaging analysis. Surg Neurol 2009;72:464–9.
6. Smith EA, Carlos RC, Junck LR, Tsien CI, Elias A, Sundgren PC. Developing a clinical decision model: MR spectroscopy to differentiate between recurrent tumor and radiation change in patients with new contrast-enhancing lesions. Am J Roentgenol 2009;192(2):45-52.
7. Goebell E, Fiehler J, Ding XQ, Paustenbach S, Nietz S, Heese O, Kucinski T, Hagel C, Westphal M, Zeumer H. Disarrangement of fiber tracts and decline of neuronal density correlate in glioma patients – a combined diffusion tensor imaging and ^{1}H-MR spectroscopy study. Am J Neiroradiol 2006;27:1426-31.
8. Yamasaki F, Sugiyama K, Ohtaki M, Takeshima Y, Abe N, Akiyama Y, Takaba J, Amatya VJ, Saito T, Kajiwara Y, Hanaya R, Kurisu K. Glioblastoma treated with postoperative radio-chemotherapy: prognostic

value of apparent diffusion coefficient at MR imaging. Eur J Radiol 2010;73(3):532-7.

9. Yamasaki F, Kurisu K, Kajiwara Y, Watanabe Y, Takayasu T, Akiyama Y, Saito T, Hanaya R, Suqiyama K. Magnetic resonance spectroscopic detection of lactate is predictive of a poor prognosis in patients with diffuse intrinsic pontine glioma. Neuro Oncol 2011;13(7):791-801.
10. Golby AJ, Kindlmann G, Norton I, Yarmarkovich A, Pieper S, Kikinis R. Interactive diffusion tensor tractography visualization for neurosurgical planning. Neurosurgery 2011;68(2):496-505.
11. Marcus CD, Marcus VL, Cucu C, Bouché O, Lucas L, Hoeffel C. Imaging techniques to evaluate the response to treatment in oncology: current standards and perspectives. Crit Rev Oncol Hemat 2009;72:217–38.
12. Louis DN, Ohgaki H, Wiestler OD, Cavenee WK, Burger PC, Jouvet A, Scheithauer BW, Kleihues P. The 2007 WHO classification of tumours of the central nervous system. Acta Neuropathol 2007;114:97–109.
13. Catani M, Schotten MT. A diffusion tensor imaging tractography atlas for virtual in vivo dissections. Cortex 2008;44:1105-32.
14. Repeatability. Behavioral Ecology Fall 2001 [cited 2012 Sept 14]. Available from: URL: www.csun.edu/~dgray/BE528/Repeatability.doc
15. Measey GJ, Silva JB, Di-Bernardo M. Testing for repeatability in measurements of length and mass in *Chthonerpeton indistinctum* (Amphibia: Gymnophiona), including a novel method of calculating total length of live caecilians. Herpetol Rev 2003;34:35–9.